

Fig. S1. FAPs number correlates with TGF- β expression and fibrosis in several skeletal muscle injury models.

(A) Representative fluorescent images of damaged (3, 7, and 14 days after glycerol injection (50% v/v)) and undamaged (day 0) tibialis anterior (TA) sections from PDGFR α ^{H2BEGFP} mice. Wheat germ agglutinin (WGA) staining (*red*) and nuclei/Höchst (*blue*) staining are also shown. (B) Quantification of the number of EGFP⁺ TA FAPs per field in acute glycerol damage. (C) Quantification of TA *TGF- β 1* mRNA expression determined by quantitative PCR in acute glycerol damage. (D) Sirius Red staining in TA sections of the glycerol damage time course. *Right*, quantification of tissue fibrosis as a percentage of total collagen (Sirius Red) stained area in acute glycerol damage. (E) Representative fluorescent images of gastrocnemius muscle 2-weeks post denervation. (F) Quantification of the number of EGFP⁺ gastrocnemius FAPs per field after 2-weeks of denervation. (G) Quantification of *TGF- β 1* mRNA expression in gastrocnemius determined by quantitative PCR after 2-weeks of denervation. (H) Sirius Red staining in gastrocnemius sections of contralateral or denervated muscle. *Right*, quantification of tissue fibrosis as a percentage of total collagen (Sirius Red) stained area. (I) Representative fluorescent images of 5-month-old PDGFR α ^{H2BEGFP} and *mdx*;PDGFR α ^{H2BEGFP} diaphragm muscle. (J) Quantification of the number of EGFP⁺ diaphragm FAPs per field. (K) Quantification of *TGF- β 1* mRNA expression in diaphragm determined by quantitative PCR. (M) Sirius Red staining in diaphragm sections. *Below*, quantification of tissue fibrosis as a percentage of total collagen (Sirius Red) stained area. (N) Representative fluorescent images of *mdx* mild and severe dystrophic phenotypes of diaphragm sections from 5-month-old PDGFR α ^{EGFP} and *mdx*;PDGFR α ^{EGFP} mice. (L) Fibro/adipogenic progenitors number correlate positively with TGF- β 1 expression and the severity of fibrosis. Scale bars: 50 μ m. Glycerol (A), denervation (E), and *mdx* mice (I). ***P < 0.001, **P < 0.005, *P < 0.05, n.s not significant; n = 3. One-Way ANOVA with Dunnett post-test and two-tailed Student's t-test.

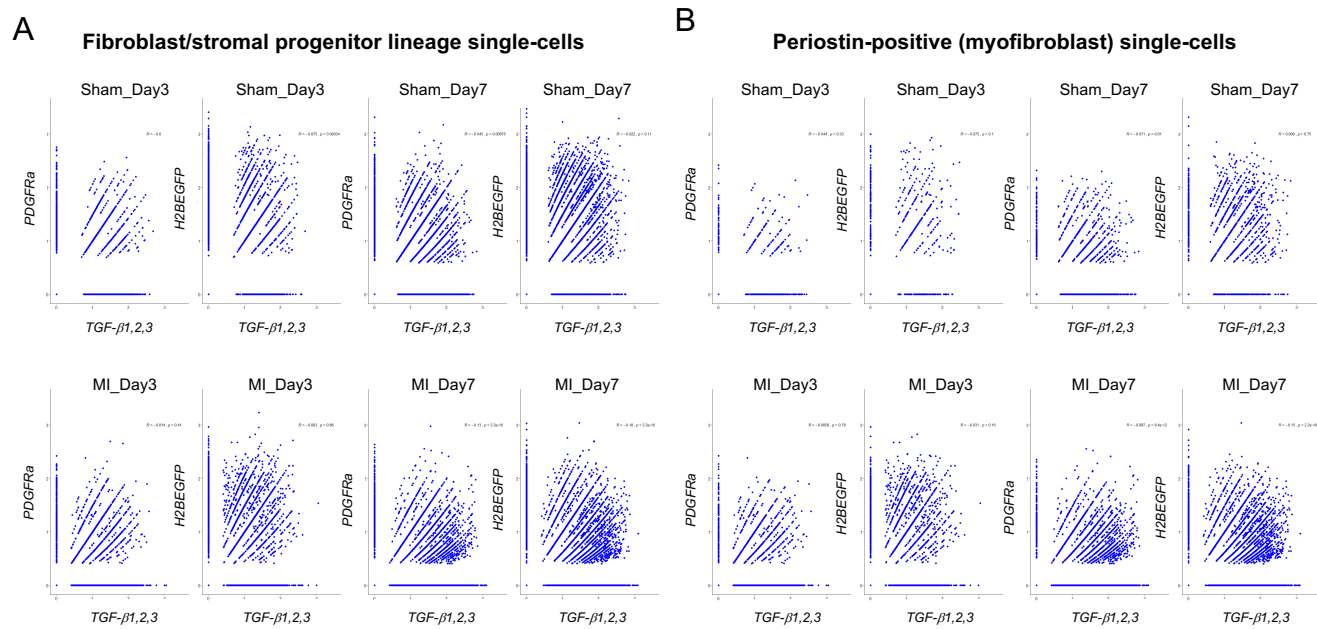


Fig. S2. Damage and TGF- β -induced cell state negatively correlate with PDGFR α expression in cardiac fibroblast/stromal progenitors.

(A) Single-cell RNA sequencing expression values, showing the relationship between PDGFR α and TGF- β cytokine (1, 2 and 3 ligands) expression in the *Pdgfra*EGFP⁺ cardiac fibroblast/stromal progenitor lineage from murine hearts at days 3 and 7 post-sham or myocardial infarction (MI) surgery. (B) This time, only the cells that express at least one count of *Postn* (Periostin) are kept. PDGFR α expression negatively correlates with TGF- β expression at day 7 of MI, which corresponds with myofibroblast differentiation (Periostin-expressing cells) occurring at that time point.

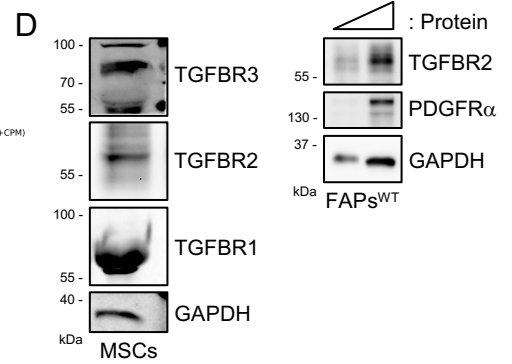
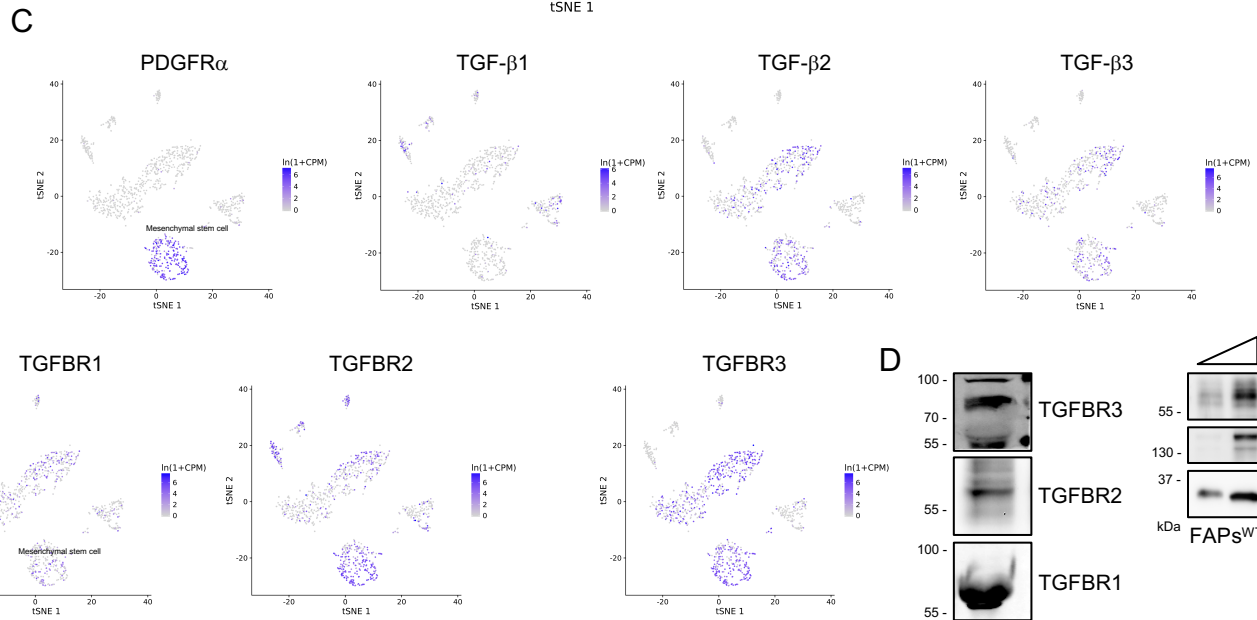
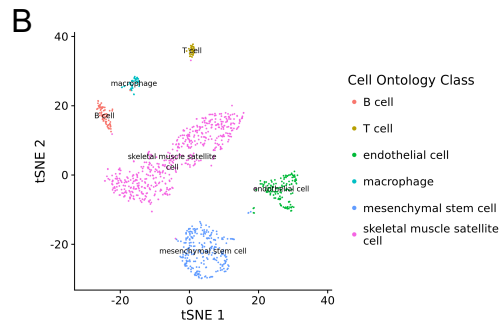
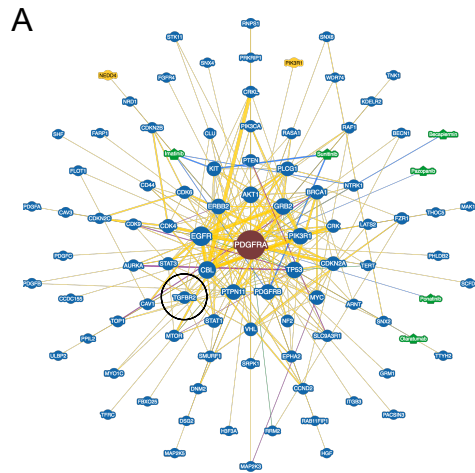


Fig. S3. TGF- β ligands and TGF-BRs are expressed by skeletal muscle stromal mesenchymal progenitors.

(A) BioGRID interactome analysis of the human PDGFR α . Black circle marks the protein-protein interaction between TGF-BR2 and PDGFR α . (B) A t-SNE plot of all cells collected using the microfluidic-droplet method, colored by the predominant cell type that composes each cluster. Cells were colored by cell type for limb muscle and visualized with t-SNE. Cell types were determined by differential gene expression of known markers between clusters. (C) t-SNE visualization of select genes (PDGFR α , TGF- β 1, TGF- β 2, TGF- β 3, TGF-BR1, TGF-BR2, and TGF-BR3) (from *grey*, low expression, to *blue*, high expression). (D) Western blot analysis of C3H/10T1/2 MSCs and wild type FAPs total lysate, showing TGF-BR1, TGF-BR2, TGF-BR3, PDGFR α , and GAPDH levels.

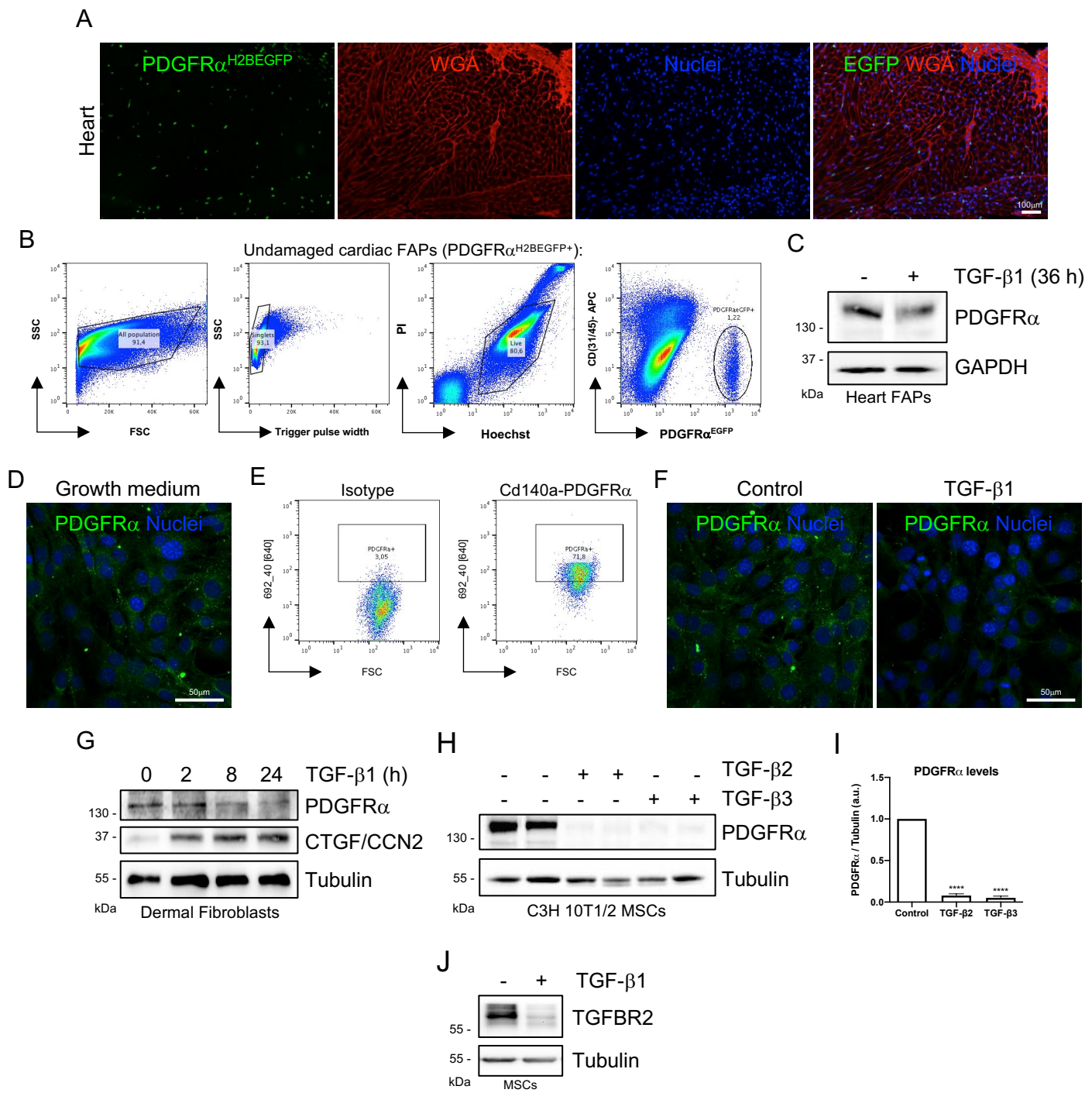


Fig. S4. TGF- β downregulates PDGFR α in heart FAPs and C3H 10T1/2 MPs.

(A) Representative fluorescent images of heart sections from PDGFR α ^{H2BEGFP} mice stained for WGA (red). (B) The sequential gating strategy used to isolate EGFP⁺ cardiac FAPs/fibroblasts from the reporter mice PDGFR α ^{H2BEGFP}. (C) PDGFR α and GAPDH levels were analyzed by western blot in heart FAPs isolated by FACS and cultured with TGF- β 1 (5 ng/ml) for 36 h. (d) Confocal image of PDGFR α immunofluorescence in proliferating C3H/10T1/2 MSCs. (E) Flow cytometry analysis of plasma membrane-bound CD140a (PDGFR α) in C3H/10T1/2 MSCs. (F) Confocal images of PDGFR α immunofluorescence, showing its cytoplasmic and plasma membrane distribution in control and TGF- β 1-treated (5ng/ml) C3H/10T1/2 MSCs for 24 h. (A, D, F) Nuclei are stained with Hoechst (blue). (G) Representative western blot analysis showing PDGFR α and CTGF/CCN2 expression levels in primary mouse dermal fibroblasts (MDFs) after treatment with TGF- β 1 (5 ng/ml) at different time points (0, 2, 8, and 24 h). Tubulin was used as the loading control. (H) Representative western blot from three independent experiments, showing PDGFR α protein levels after stimulation with TGF- β 2 and TGF- β 3 for 24 h at a final concentration of 5 ng/ml in MSCs. Tubulin was used as the loading control. (I) Quantification of PDGFR α expression after treatment with TGF- β 2 and TGF- β 3. N=3; ****P < 0.0001; One-Way ANOVA with Dunnett post-test. (J) TGF-b1 reduces TGF-b receptor type II expression. Representative western blot analysis showing TGF-BR2 expression levels in C3H/10T1/2 cells after TGF-b1 (5 ng/ml) treatment for 24 h. Tubulin was used as the loading control.

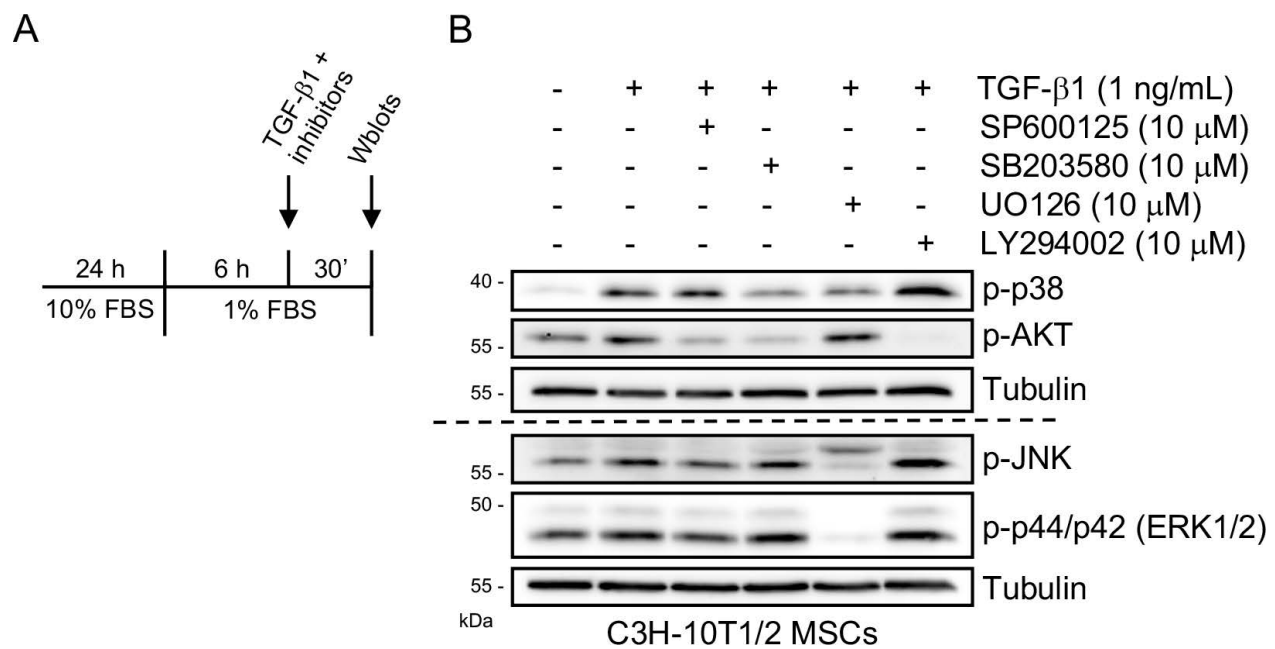


Fig. S5. TGF- β 1-mediated signaling pathways in mesenchymal progenitors.

(A) Outline of C3H/10T1/2 MSCs, TGF- β signaling pathway inhibitors, and TGF- β 1 treatment (1 ng/ml) protocol. (B) Representative western blot of phosphorylated (p-) p38, p-AKT, p-JNK, p-ERK1/2, and tubulin from C3H/10T1/2 MSCs treated with TGF- β 1 and SP600125 (JNK), SB203580 (p38), UO126 (ERK1/2), LY294002 (PI3K/AKT) inhibitors. Tubulin was used as the loading control.

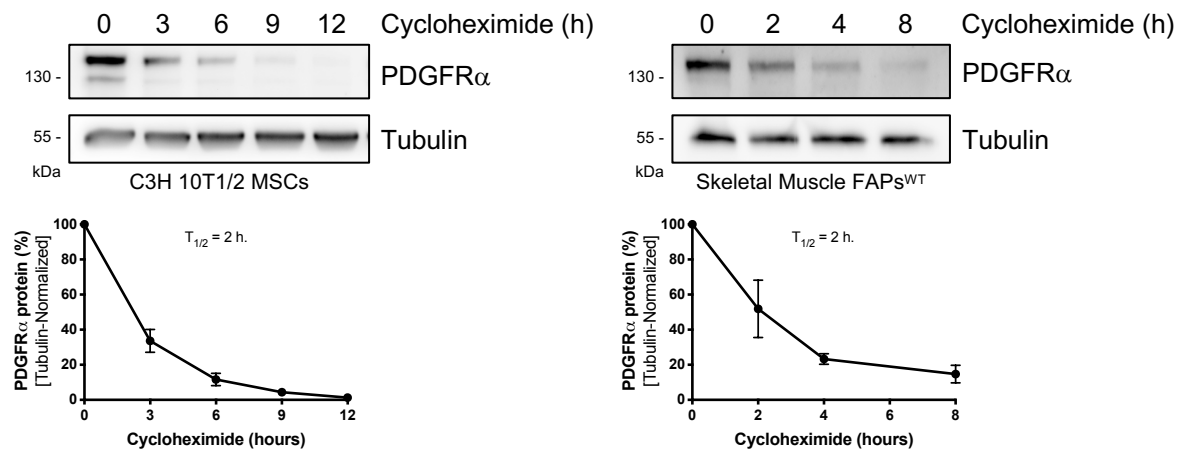


Fig. S6. Evaluation of PDGFR α protein half-life in mesenchymal stromal cells and fibro/adipogenic progenitors.

Representative western blot of PDGFR α and tubulin in C3H/10T1/2 MSCs (*left*) and skeletal muscle FAPs (*right*) after a time course treatment with cycloheximide 30 μ g/ml. Quantifications of PDGFR α protein levels (tubulin-normalized) during the cycloheximide time course (*lower graphs*).

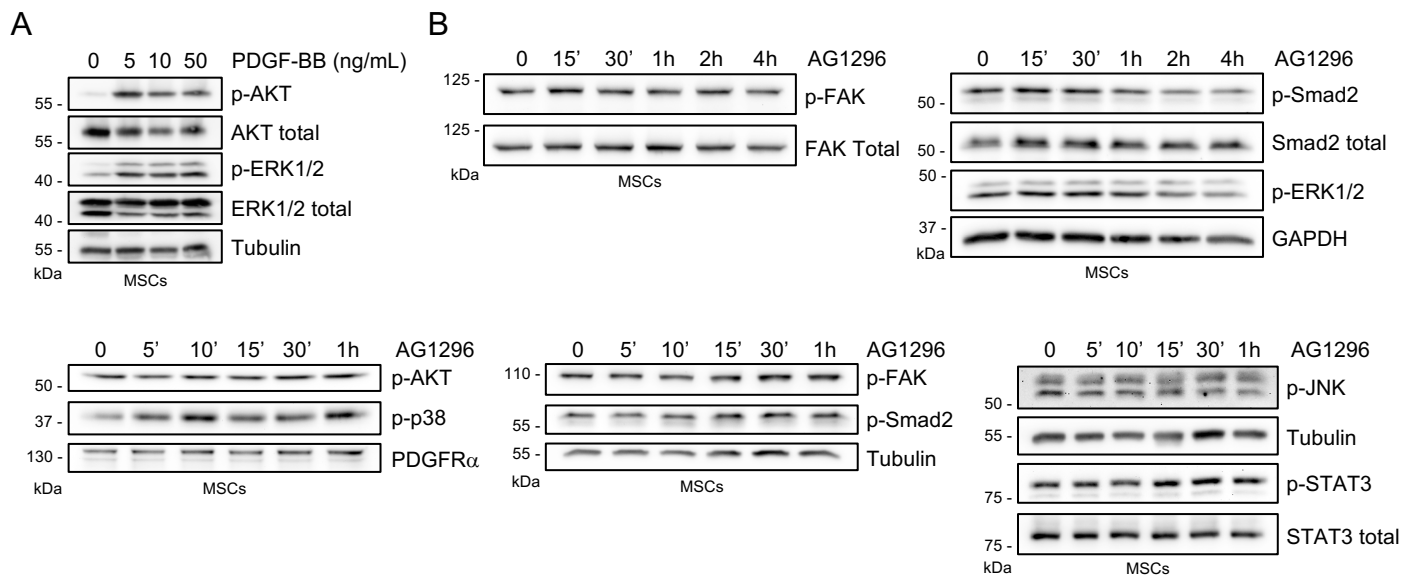


Fig. S7. Evaluation of signaling pathways activated by PDGF-BB stimulation and AG1296 inhibitory effects in mesenchymal stromal cells.

(A) Representative western blot analysis showing phosphorylated levels of AKT and ERK1/2 after PDGF-BB treatment (20 ng/ml). AKT and ERK1/2 were used as total proteins. Tubulin was used as the loading control. (B) Representative western blot analysis showing phosphorylated levels of FAK, Smad2, and ERK1/2 after AG1296 treatment (10 μ M). FAK, Smad2, and GAPDH were used as total proteins. (C) Representative western blot analysis showing phosphorylated levels of AKT, p38, FAK, Smad2, JNK, and STAT3 after AG1296 treatment (10 μ M). PDGFR α , tubulin, and STAT3 were used as total proteins.

Fig. S8. The PDGFR α pharmacological inhibitor AG1296 impairs TGF- β -mediated ECM remodeling and Smad2 signaling.

(A) Bright-field images showing TGF- β 1-induced myofibroblast differentiation of C3H/10T1/2 MSCs after 24 h of treatment. (B) Z-stack confocal images showing the ECM organization of fibronectin (Fn) and filamentous actin (F-actin) in control and TGF- β 1-induced myofibroblast differentiation. (C) Z-stack confocal images showing the ECM organization of fibronectin (Fn) and filamentous actin (F-actin) in control, AG1296, TGF- β 1, and AG1296 + TGF- β 1 treated C3H 10T1/2 cells. Scale bars: 50 μ m. Nuclei are stained with H \ddot{o} chst (*blue*). (D) Representative western blot analyses showing phosphorylated levels of the TGF- β canonical effector Smad2 after TGF- β 1 and AG1296 treatments (different concentrations) at 30 minutes. Tubulin and GAPDH were used as the loading controls. (E) Representative western blot analyses showing phosphorylated levels of the TGF- β canonical effector Smad2, AKT, and ERK1/2 after TGF- β 1 and PDGF-BB treatments. Total protein forms were used as the loading controls. PDGFR α protein levels were used as a positive control of TGF- β -mediated effects.

Table S1. The expression of the PDGFR α immediate early gene *Txnip* decreases during skeletal muscle regeneration.

In-silico analysis from microarray data obtained from Lukjanenko et al., 2013. Skeletal muscle *Txnip* expression decreases at days 3 and 7 after acute damage.

Probe set ID	Gene Symbol	Gene Name	Glycerol 3 days - Sham 14 days_logFC	Glycerol 3 days - Sham 14 days_log.adj.P.Val
1415997_at	<i>Txnip</i>	thioredoxin interacting protein	-1.73	4.51
Probe set ID	Gene Symbol	Gene Name	Glycerol 7 days - Sham 14 days_logFC	Glycerol 7 days - Sham 14 days_log.adj.P.Val
1415997_at	<i>Txnip</i>	thioredoxin interacting protein	-1.2	2.54
Probe set ID	Gene Symbol	Gene Name	Cardiotoxin 3 days - Sham 14 days_logFC	Cardiotoxin 3 days - Sham 14 days_log.adj.P.Val
1415997_at	<i>Txnip</i>	thioredoxin interacting protein	-1.63	3.45
Probe set ID	Gene Symbol	Gene Name	Cardiotoxin 7 days - Sham 14 days_logFC	Cardiotoxin 7 days - Sham 14 days_log.adj.P.Val
1415997_at	<i>Txnip</i>	thioredoxin interacting protein	-1.79	4.17

Table S2: Primers used in RT-qPCR

Gene	Forward primer (5'-3')	Reverse primer (5'-3')
<i>Txnip</i>	ACGACTCTCAAGACAGCCC	GGAGTTCAAGCAGAGAGGCA
<i>Tiparp</i>	CAGTTGCGGCTTTCAGCGCTCAG	CTCAAGGATCTCAGGGTCCAGTTC
<i>Axud1</i>	GTCTGTCCTCGGCTGTTGGAACC	CCACCTCAGCATCTCCAGCTTC
<i>Arid5b</i>	CAGTACTGTCCGTACCGGTCCATG	GTTCCATCTGCCCTGCATTCTTCGCC
<i>Schip1</i>	GCACAATGGCAACGTGGTGGTAGC	CCGTCTTACTGTCATCTGCATCGCTG
<i>Tgfb1</i>	CTCCACCTGCAAGACCAT	CTTAGTTTGGACAGGATCTGG
<i>Adiponectin</i>	GGAACCTTGTGCAGGTTGGAT	TCTCCAGGAGTGCCATCTCT
<i>Pparg</i>	AGGCGAGGGCGATCTTGACAG	AATTCGGATGGCCACCTCTTTG
<i>18S</i>	TGACGGAAGGGCACCACCAG	CACCACCACCCACGGAATCG